Linear Stability Analysis of Poiseuille-Bénard-Marangoni Flow in a Horizontal Infinite Liquid Film

Lahcen Bammou, Serge Blancher, Yves Le Guer, Kamal El Omari, Brahim Benhamou

Linear stability analysis of Poiseuille–Bénard–Marangoni flow in a horizontal infinite liquid film

Lahcen Bammou[a], Serge Blancher[a], Yves Le Guer[a], Kamal El Omari[a], Brahim Benhamou[b]

[a]Laboratoire des Sciences de l'Ingénieur Appliquées la Mécanique et au gènie Electrique (SIAME), Fédération IPRA-CNRS, Université de Pau et des Pays de l'Adour, Pau, France

[b]Laboratoire de Mécanique des Fluides et d'Energétique (CNRST-URAC27), Université Cadi Ayyad — Dépt. de Physique, Faculté des Sciences Semlalia, Marrakech, Maroc

We present the first linear stability analysis of a Poiseuille–Bénard–Marangoni flow, which refers to a horizontal infinite liquid film flowing in one direction with uniform heating from below. This study concerns the two limiting cases of pure buoyancy effect ($Ma = 0$) and pure thermocapillary effect ($Ra = 0$). The stability thresholds of the flow and their variation with the control parameters (Biot, Reynolds and Prandtl numbers) are given and compared with those for a Poiseuille–Rayleigh–Bénard flow. The spatial structures of the flow are presented, and it is shown that the centers of the rolls are shifted upwards compared to the PRB case and that there is a loss of symmetry with respect to the vertical axis for the transverse rolls. These effects are directly linked to thermocapillary convection.

1. Introduction

The development of longitudinal rolls has long been observed in different fluid flow configurations. The formation of cloud streets in planetary boundary layers [1] and the Görtler vortices that appear along concave boundary layers [2] are sample manifestations of these longitudinal rolls. Another flow that leads to the formation of such patterns has received extensive attention in the literature: the Poiseuille–Rayleigh–Bénard (PRB) flow. This system results from the combination of the buoyancy instability of a confined horizontal fluid layer heated from below and a mean flow [3]. The introduction of a mean flow to the buoyancy thermocapillary instability (i.e. the Rayleigh–Bénard–Marangoni flow [4,5]) leads to a novel system called the Poiseuille–Bénard–Marangoni (PBM) flow, which is the subject of the present study. This system is not only of a great interest for industrial applications such as the cooling by liquid films; but it may also serve as a framework for the study of the formation of such flow instabilities. Various linear and weakly nonlinear stability analyses of PRB flow have been conducted in channels of both infinite and finite transversal extensions [6,7]. The onset of a secondary flow, in the form of longitudinal rolls, occurs at a critical Rayleigh number of approximately $Ra_c = 1708$ [8]. The critical Rayleigh number Ra_c and the critical wave number k_y in the spanwise direction are shown to be independent of the Reynolds number Re. The existence of unsteady transverse thermoconvective rolls with axes perpendicular to the main flow has been demonstrated by Luijkx et al. [9]. For smaller Reynolds numbers, the critical Rayleigh number corresponding to the onset of transverse rolls has been found to be a function of both the channel aspect ratio and the Prandtl number [10,6]. When a free liquid surface is present, the surface tension variation resulting from the temperature gradient along the surface may induce motion within the fluid, called thermocapillary flow. The investigation of the thermocapillary effect has been mostly considered in thin liquid layers flowing down an inclined, uniformly [11] or non-uniformly [12] heated plate. In our previous numerical simulation study [13], we showed that the introduction of the thermocapillary effect on the mixed convection changes the rotation direction of the rolls near the side walls of the channel and promotes heat transfer.

Most of the studied flow situations involving thermocapillary forces are those where no forced convection (main stream) is present. These flows, referred to as Bénard–Marangoni flows, have been extensively studied in the literature [14–17]. Pearson (1958) is commonly recognized to be the first researcher to propose a linear stability analysis of the thermocapillary flow within a horizontal fluid layer with a free surface considered as non-deformable [18]. Pearson modeled the presence of the upper gas layer through an adequate boundary condition that takes also into account the heat transfer. Using this model, Pearson established the critical condition (critical Marangoni number) beyond which the liquid layer becomes unstable. Scriven and Sternling [19] extended this work to the case of a deformable free surface and demonstrated that, in this particular case, the liquid layer is always unstable and that there is no critical Marangoni number. Later, the conjugated

☆ Communicated by W.J. Minkowycz.

* Corresponding author.
E-mail address: lahcen.bammou@gmail.com (L. Bammou).

role of buoyancy forces has been investigated by Laure and Roux [20] for low Prandtl number (Pr) liquids, while Parmentier et al. [21] studied liquids with Pr up to 10. Burguete et al. [22] analyzed the destabilization of the thermocapillary–buoyancy flows toward different patterns, depending on the temperature difference ΔT and on the liquid pool depth d. For example, hydrothermal waves were observed for small values of d, while for larger values, stationary longitudinal rolls were observed. The transition of the buoyant–thermocapillary instabilities from oscillatory to stationary modes has been showed by Mercier and Normand [23]. This transition occurs when the Bond number (the ratio between the Rayleigh and the Marangoni numbers) is increased.

Concerning the convective and absolute instability studies, Müller et al. [24,25] have first determined the transition curve between the convective and absolute instability zones for the transverse rolls by using a weakly nonlinear theory based on a Ginzburg–Landau equation. Ouazzani et al. [10,26], experimentally, and Nicolas et al. [27], numerically, have shown that the transition between the basic flow and the transverse rolls exactly corresponds to the absolute/convective instability boundary curve, provided that the flow is not continuously perturbed at the inlet. Furthermore, for an infinite extent system and, by evaluating the long-time behavior of the Green function in the horizontal plane, Carrière and Monkewitz [28] theoretically revealed that the mode reaching zero group velocity at the convective/absolute transition always corresponds to transverse rolls, while the system remains convectively unstable with respect to pure longitudinal rolls for all nonzero Reynolds numbers.

In this paper, we present the first linear stability analysis of a horizontal infinite liquid film flowing in one direction with uniform heating from below. We limit our study in this paper to the two limiting cases of $Ma = 0$ (pure buoyancy effect) and $Ra = 0$ (pure thermocapillary effect). An eigenvalue problem is obtained through this analysis and is solved numerically using the Chebyshev collocation spectral method. We provide results for the critical dimensionless parameters of the thermoconvective instabilities. Both longitudinal and transverse rolls are studied, and their spatial structures are given. A comparison with the PRB flow is given to illustrate the influence of the free upper surface on both the critical parameters and the development of spatial structures.

2. Physical model

Our study system consists of an infinite horizontal liquid film of height H flowing in one direction (see Fig. 1). The bottom wall is kept at a constant and uniform temperature T_h that is higher than the initial temperature of the liquid T_0. The temperature of the gas over the liquid layer is also fixed at T_0. Assuming an incompressible Newtonian fluid and considering the Boussinesq approximation, the three-dimensional equations governing the conservation of mass, momentum and energy are written as follows:

$$\vec{\nabla} \cdot \vec{V} = 0 \tag{1}$$

$$\frac{\partial \vec{V}}{\partial t} + \left(\vec{V} \cdot \vec{\nabla}\right)\vec{V} = -\vec{\nabla}P + \frac{2}{Re}\vec{\nabla}^2\vec{V} + \frac{Ra}{2PrRe^2}\theta\vec{z} \tag{2}$$

$$\frac{\partial \theta}{\partial t} + \vec{V} \cdot \vec{\nabla}\theta = \frac{2}{PrRe}\vec{\nabla}^2\theta. \tag{3}$$

The dimensionless parameters that appear in these equations are: the Reynolds number $Re = \frac{U_m H}{\nu}$, where U_m is the mean flow velocity and ν is the kinematic viscosity; the Rayleigh number $Ra = \frac{g\beta(T_h - T_0)H^3}{\nu\alpha}$, where g is the acceleration due to gravity, β is the fluid thermal expansion coefficient and $T_h - T_0$ is the temperature difference between the heated plate and the surrounding air; and the Prandtl number $Pr = \frac{\nu}{\alpha}$, where α is the fluid thermal diffusivity. In these equations, the half channel height $H/2$, the mean flow velocity U_m, the dynamic pressure ρU_m^2 and the ratio $H/2U_m$ are used as reference quantities for length, velocity, pressure and time, respectively. The dimensionless temperature θ is defined as $\theta = (T - T_0)/(T_h - T_0)$. At the bottom of the channel, the fluid velocity $\vec{V}$ (V_x, V_y, V_z) satisfies the no-slip condition, and the bottom wall is assumed to be isothermal ($\theta = 1$). By assuming a planar surface, a shear stress boundary condition is imposed on the free surface, as derived from the balance between the surface tension forces and the viscous stresses in the fluid ($\frac{\partial V_x}{\partial Z} = -\frac{Ma}{Pe}\frac{\partial \theta}{\partial X}$, $\frac{\partial V_y}{\partial Z} = -\frac{Ma}{Pe}\frac{\partial \theta}{\partial Y}$ and $V_z = 0$) where $Ma = \frac{\partial \sigma}{\partial T}\frac{\Delta T H}{\mu\alpha}$ and $Pe = \frac{U_m H}{\alpha}$ are the Marangoni and Péclet numbers, respectively. The surface tension coefficient is assumed to be a linear function of temperature T: $\sigma = \sigma_0 + \frac{\partial \sigma}{\partial T}(T - T_0)$. On the free surface, we use the convective thermal condition $\frac{\partial \theta}{\partial Z} = -\frac{Bi}{2}\theta$. Bi is the Biot number, defined as $Bi = \frac{hH}{\lambda}$, where h is the heat transfer coefficient and λ is the thermal conductivity of the liquid. To perform a linear stability analysis of the problem, we split $\vec{V}$, P and θ into the basic state ($\overline{\vec{V}}, \overline{P}, \overline{\theta}$) and the disturbance ($\vec{V}', P', \theta'$). In the absence of lateral boundaries, the nondimensional basic conductive steady state can be obtained and is described by a linear temperature profile and a plane half-Poiseuille velocity profile:

$$\overline{\theta}(Z) = \frac{2 + Bi}{2(Bi + 1)} - \frac{Bi}{2(Bi + 1)}Z \tag{4}$$

$$\overline{V_x}(Z) = -\frac{3}{8}\left(Z^2 - 2Z - 3\right). \tag{5}$$

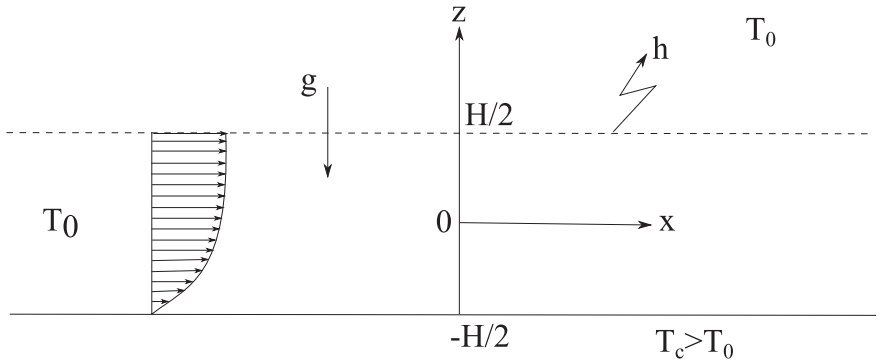

Fig. 1. The study configuration and corresponding boundary conditions.

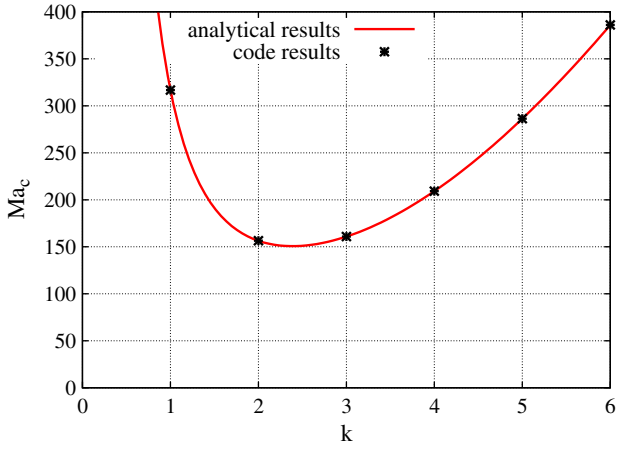

Fig. 2. Comparison of the numerical results of neutral stability curve with the analytical results [18,33] for $Ra = 0$, $Bi = 2$ and $Pr = 7$.

We assume the three-dimensional infinitesimal perturbations to be in the form of normal modes:

$$\left(V_x', V_y', V_z', P', \theta'\right) = \left(\hat{V}_x, \hat{V}_y, \hat{V}_z, \hat{P}, \hat{\theta}\right) e^{i\left(k_x X + k_y Y - \sigma t\right)} \tag{6}$$

where k_x and k_y are the wave numbers of the disturbance in the x- and y-directions and σ is the complex pulsation. A linear stability analysis of Eqs. (1), (2) and (3) leads to the following two ODEs for the amplitude of the normal modes of the vertical velocity component disturbance, $\hat{V}_z$, and the temperature disturbance, $\hat{\theta}$:

$$\frac{2}{Re}\left(D^2 - k^2\right)^2 \hat{V}_z = i\left[\left(k_x \overline{V} - \sigma\right)\left(D^2 - k^2\right) - k_x D^2 \overline{V}\right]\hat{V}_z + \frac{Ra}{2PrRe^2} k^2 \hat{\theta} \tag{7}$$

$$-i\sigma\hat{\theta} + ik_x \overline{V}\hat{\theta} + \hat{V}_z D\overline{\theta} = \frac{2}{PrRe}\left(D^2 - k^2\right)\hat{\theta} \tag{8}$$

with the following boundary conditions:

$$\hat{V}_z = 0, \quad D\hat{V}_z = 0, \quad \hat{\theta} = 0 \qquad \text{at} \quad Z = -1 \tag{9}$$

$$\hat{V}_z = 0, \quad D^2\hat{V}_z + k^2 \frac{Ma}{Pe}\hat{\theta} = 0, \quad D\hat{\theta} + \frac{Bi}{2}\hat{\theta} = 0 \qquad \text{at} \quad Z = 1 \tag{10}$$

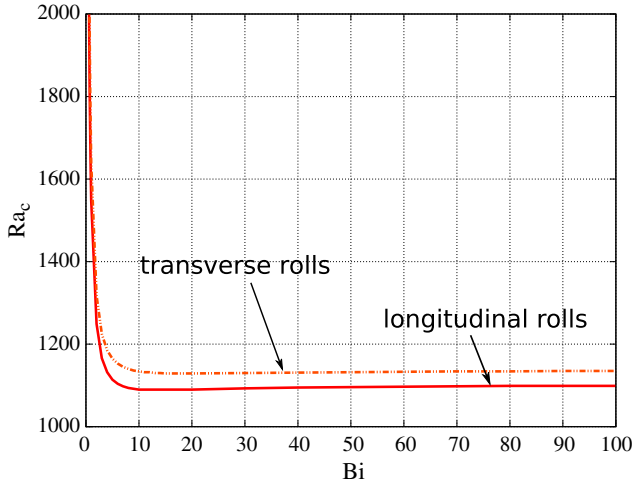

Fig. 3. Critical Rayleigh number as a function of the Biot number: Pure buoyancy effect ($Ma = 0$, $Re = 15$, $Pr = 7$).

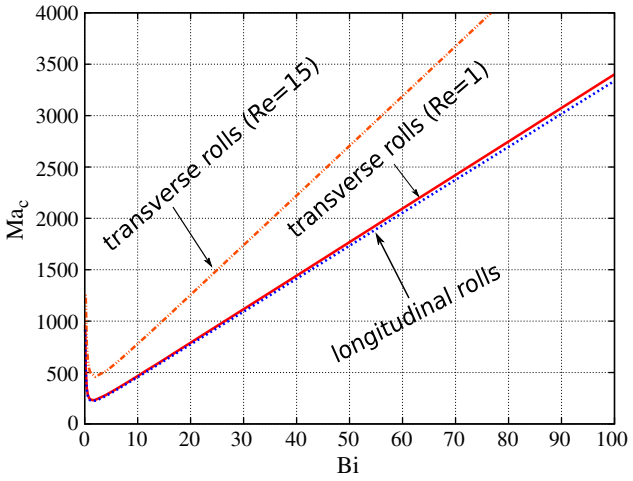

Fig. 4. Critical Marangoni number as a function of the Biot number: Pure thermocapillary effect ($Ra = 0$, $Re = 1$ and 15, $Pr = 7$).

where $k^2 = k_x^2 + k_y^2$ and $D = \partial/\partial Z$. Eq. (7) is a linear fourth-order ODE that reduces to the classical Orr–Sommerfeld equation when $Ra = 0$ [29], and Eq. (8) is a linear second-order ODE for the energy perturbation. These two equations along with the boundary conditions Eqs. (9–10) describe an eigenvalue problem in which σ is the eigenvalue. The above framework allows for a numerical calculation of the dispersion relation:

$$\mathcal{D}\left(k_x, k_y, \sigma, Ra, Ma, Bi, Re, Pr\right) = 0. \tag{11}$$

This dispersion relation is obtained numerically by discretizing the eigenvalue problem using the Chebyshev spectral collocation method [30,31]. To determine the critical thresholds of the problem, the eigenvalues of the system Eqs. (7–10) are placed in a decreasing order of the imaginary part of σ. When $Imag(\sigma)$ becomes positive, the basic state is unstable.

3. Validation of the numerical method

The calculation code is implemented in MATLAB. It has been thoroughly tested against analytical and other numerical results. The present developments being original, there is no previous similar work in the literature to make comparisons. Thus we proceeded in two steps. First we validated the implementation of the Eqs. (7) and (8) and in a second step we validated the boundary conditions Eqs. (9–10). The first

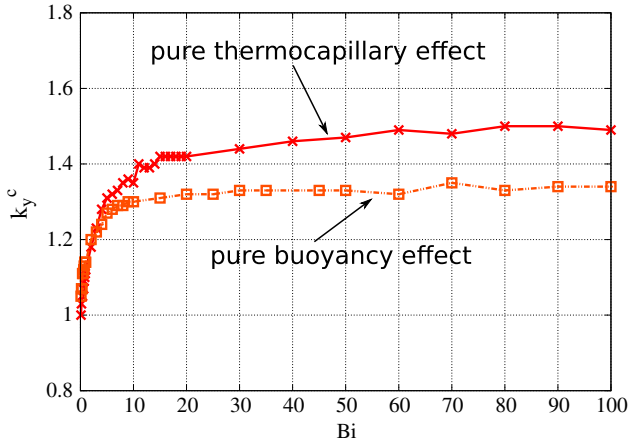

Fig. 5. Critical spanwise wave number k_y^c of longitudinal rolls as a function of the Biot number ($Pr = 7$ and $Re = 15$).

Table 1
Comparison of the critical Rayleigh number Ra_c and the critical wave number k_y^c for the onset of longitudinal rolls for free-surface flow with those obtained from numerical results for a PRB flow.

	Free-surface flow ($Bi = 100$ and $Ma = 0$)	PRB flow
Ra_c	1097.0	1707.8
k_y^c	1.34	1.56

validation concerns the stability of the Poiseuille–Rayleigh–Bénard flow in infinite lateral extension ducts heated uniformly from below. In this case, the modeled configuration has the same governing equations (Eqs. (7) and (8)) but with a rigid boundary condition in place of the free flat surface [32]. The stability criteria for the onset of longitudinal rolls are obtained and compared with those published previously in the literature [32,3]. Our results agree well with the literature and show that the basic flow becomes unstable towards the longitudinal rolls at the critical Rayleigh number $Ra_c = 1707.8$ and for a critical wave number $k_y = 1.558$ (k_y being scaled here by $H/2$). These values are independent of the Reynolds number. The second validation test case concerns the Marangoni convection within an infinite fluid layer heated from below and with a convective heat exchange at the free surface. In this case we kept our boundary conditions (Eqs. (9) and (10)) but with different governing equations (absence of forced and natural (buoyancy) convection) [33]. We represent in Fig. 2 the neutral stability curve for the thermoconvective instability as a function of the wavenumber k for $Bi = 2$. Our results are in good agreement with those obtained analytically by Pearson [18] and Colinet et al. [33].

4. Results and discussion

In this flow situation, two mechanisms are responsible for the onset of thermoconvective patterns: buoyancy and thermocapillary convection. In this letter, we focus on the thermal convective instabilities in the form of longitudinal rolls ($k_x = 0, k_y \neq 0$, $Real(\sigma) = 0$) and transverse rolls ($k_x \neq 0$, $k_y = 0$, $Real(\sigma) \neq 0$). Figs. 3 and 4 show the evolution of the critical parameters (Ra_c and Ma_c respectively) for the development of longitudinal and transverse rolls according to the Biot number in the limiting cases of pure buoyant convection and pure thermocapillary convection. In both cases, the flow is always stable at $Bi = 0$ due to the constant basic state temperature $\overline{\theta}(Z) = 1$, which corresponds to the case of a free surface acting as an insulating surface. In the case of pure buoyant convection (Fig. 3), as the Biot number increases, the critical Rayleigh number initially decreases steeply and then increases slowly towards an asymptotic value ($Ra_c = 1097$ for longitudinal rolls and $Ra_c = 1135$ for transverse rolls). These two values of

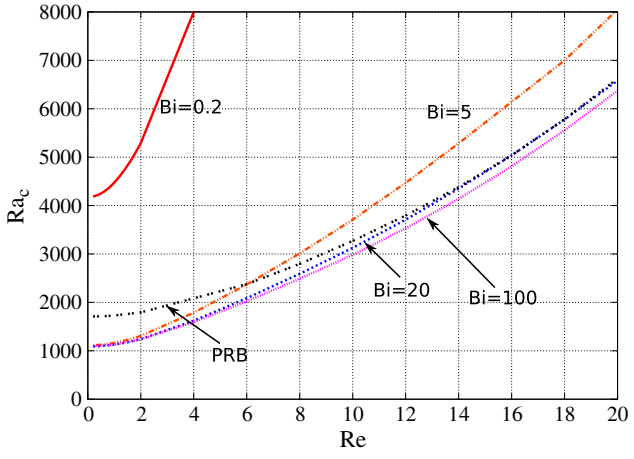

Fig. 6. Evolution of the critical Rayleigh number Ra_c for the onset of transverse rolls as a function of Re for different Bi ($Pr = 7$, $Ma = 0$). Comparison with the case of PRB flow.

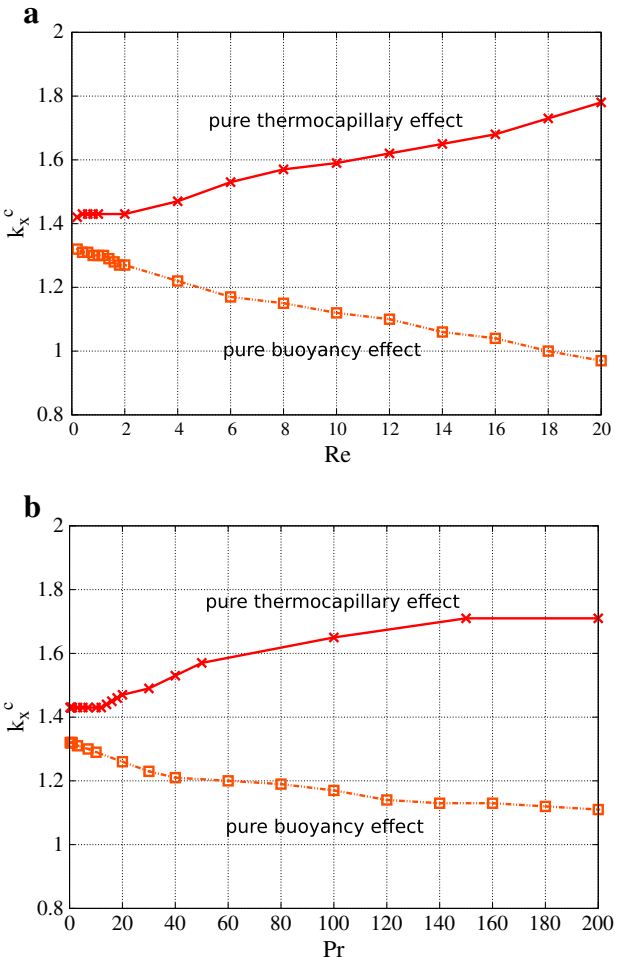

Fig. 7. Critical streamwise wave number of the transverse rolls as a function of: (a) Reynolds number Re ($Pr = 7$ and $Bi = 20$) and (b) Prandtl number Pr ($Re = 1$ and $Bi = 20$).

Ra_c enclose the classical value founded for a static fluid layer with a zero stress free surface and an infinite Bi number (see for example Kundu and Cohen, 2002 [34]). This behavior can be explained by the thermal boundary condition at the free surface, which affects the temperature perturbations in the bulk flow. Indeed, for small Bi values, these perturbations are very sensitive to the heat transfer at the free surface. For large Bi values, the free surface can be regarded as an imposed constant temperature that causes the critical Rayleigh number to approach this asymptotic value. We observe that the longitudinal rolls induced by the buoyancy effect appear first because the critical Rayleigh number for the longitudinal rolls is always smaller than that for the transverse rolls. This result has also been found for PRB flow in channels of infinite lateral extension [3]. In the case of pure thermocapillary convection (Fig. 4), the critical Marangoni number decreases steeply until the Biot number reaches a value of approximately $Bi = 1.5$, after which the critical Marangoni number then increases linearly with Bi. This behavior occurs because for low Bi values (not $Bi = 0$), the free surface temperature is not homogeneous, which favors horizontal temperature gradients and this induces the thermocapillary instabilities. However, for large Bi values, the temperature tends to be homogenized at the free surface which reduces the horizontal temperature gradients thus the thermocapillary instabilities. When the instabilities are induced by pure thermocapillary effects, the critical Marangoni number is approximately equal for both types of instabilities for small Reynolds numbers, while the longitudinal rolls appear first for large Reynolds numbers.

Fig. 5 shows the effect of the Biot number on the critical wave number k_y^c of the longitudinal rolls in the case of pure buoyancy effect and in the case of pure thermocapillary effect. We observe that k_y^c

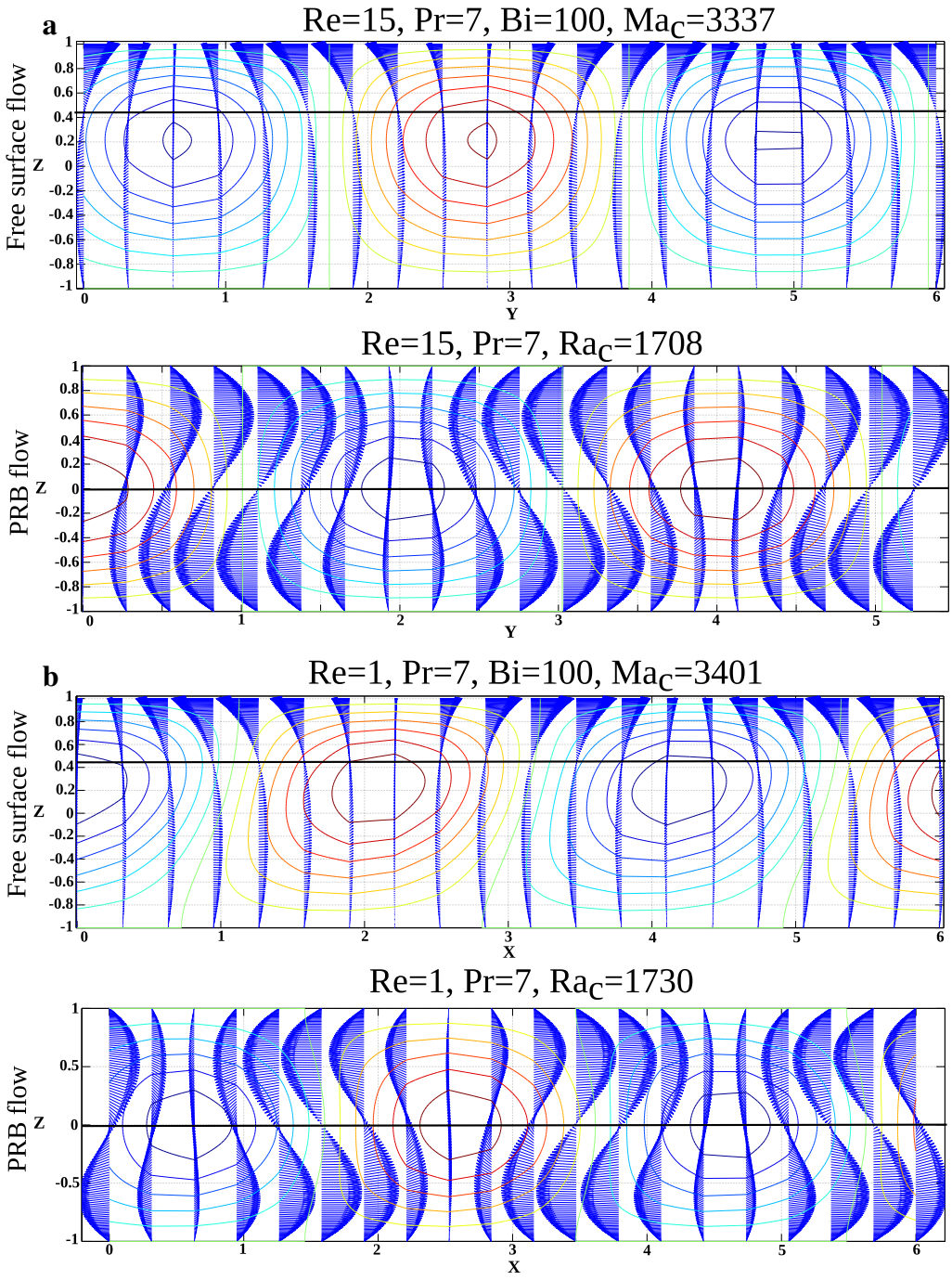

Fig. 8. Cross sections of $\vec{V}$ components (arrows) and $\hat{\theta}$ (contours) of the most unstable eigenmode. Free-surface ($Ra = 0$) compared to the PRB flow. (a) Longitudinal rolls. (b) Transverse rolls.

gradually increases with Bi to reach an almost constant value of $k_y^c = 1.34$ in the case of pure buoyancy effect and $k_y^c = 1.50$ in the case of pure thermocapillary effect. Thus, for large Biot numbers, thermocapillary forces generate more convective longitudinal rolls than buoyancy forces: the thermocapillary forces are weak, which reduces the wavelength of the rolls. Comparing these results with the PRB flow (see Table 1), we note that the upper rigid surface stabilizes the flow and delays the onset of longitudinal rolls by increasing Ra_c. The presence of an upper wall also increases the critical spanwise number ($k_y^c(\mathrm{PRB}) > k_y^c$), which means that more convective rolls arise in the case of the PRB flow than with a free surface.

As for the PRB flow [8], in our flow situation, the critical values (Ra_c and Ma_c) for the onset of stationary longitudinal rolls are independent of the Reynolds and Prandtl numbers. However, the critical values for the onset of transverse rolls are dependent on the Reynolds and Prandtl numbers. Comparing with the PRB flow, it is apparent from Fig. 6 that the free-surface flow is always more stable than the PRB flow for small Biot numbers regardless of the Re value. However, for moderate Biot numbers ($Bi < 20$), the free-surface flow is less stable compared to the PRB flow at low Re but becomes more stable compared to the PRB flow for large Re. In the case of large Biot numbers, the free-surface flow is always unstable compared to the PRB flow regardless of Re.

Fig. 7(a) and (b) shows the evolution of the critical wave number for the transverse rolls k_x^c as a function of Re and Pr, respectively, in the cases of pure buoyancy and pure thermocapillary effects. The wave number of the transverse rolls due to thermocapillary effect increases as Re and Pr

increase, whereas the wave number of the transverse rolls due to the buoyancy effect decreases when *Re* and *Pr* increase. Thus, buoyancy and thermocapillary effects act in an opposing manner to establish the critical wave number k_x^c.

The flow structures for the longitudinal and transverse rolls of the free-surface flow compared to the flow with a rigid upper surface (PRB flow) are plotted in Fig. 8(a) and (b), respectively. As shown in the case of PRB flow, the rolls are centered at $Z = 0$ and have diameters close to the channel height. In the case of free-surface flow, the centers of the rolls are shifted upwards. The transverse rolls in the case of free-surface flow are slightly deformed and are no longer symmetrical with respect to the z-axis. These effects are directly linked to the thermocapillary forces exerted at the liquid surface.

5. Conclusion

To summarize, we have performed the first stability analysis of a horizontal infinite liquid film flowing in one direction with uniform heating from below. We obtained the critical parameters (Ra_c, Ma_c, k_y^c and k_x^c) for the onset of longitudinal and transverse rolls and their variations as a function of the other control parameters (*Bi*, *Re*, *Pr*). A comparison with PRB flow reveals that the upper free surface destabilizes the flow in the case of longitudinal rolls and can stabilize or destabilize the flow in the case of transverse rolls depending on the Biot and Reynolds numbers. The presence of the upper free surface also decreases the critical wave number of the rolls compared to the PRB flow. The structures of the longitudinal and transverse rolls are also modified.

Acknowledgments

This work has been supported by a PBER grant (Programme de Bourses d'Excellence de Recherche) from CNRST-Morocco and by the Volubilis program of Morocco–French cooperation (MA/09/214-Maroc, MA/09/213-France).

References

[1] J.P. Kuettner, Cloud bands in the earth's atmosphere: observations and theory, Tellus 23 (4–5) (1971) 404–426.
[2] W.S. Saric, Görtler vortices, Annu. Rev. Fluid Mech. 26 (1) (1994) 379–409.
[3] X. Nicolas, Bibliographical review on the Poiseuille–Rayleigh–Bénard flows: the mixed convection flows in horizontal rectangular ducts heated from below, Int. J. Therm. Sci. 41 (10) (2002) 961–1016.
[4] D.A. Nield, Surface tension and buoyancy effects in cellular convection, J. Fluid Mech. 19 (03) (1964) 341–352.
[5] J. Pantaloni, R. Bailleux, J. Salan, M. Velarde, Rayleigh–Benard–Marangoni instability: new experimental results, J. Non-Equilib. Thermodyn. 4 (4) (1979) 201–218.
[6] X. Nicolas, J.M. Luijkx, J.K. Platten, Linear stability of mixed convection flows in horizontal rectangular channels of finite transversal extension heated from below, Int. J. Heat Mass Transfer 43 (4) (2000) 589–610.
[7] Y. Kato, K. Fujimura, Prediction of pattern selection due to an interaction between longitudinal rolls and transverse modes in a flow through a rectangular channel heated from below, Phys. Rev. E. 62 (2000) 601–611.
[8] Y. Mori, Y. Uchida, Forced convective heat transfer between horizontal flat plates, Int. J. Heat Mass Transfer 9 (8) (1966) 803–808.
[9] J. Luijkx, J. Platten, J. Legros, On the existence of thermoconvective rolls, transverse to a superimposed mean Poiseuille flow, Int. J. Heat Mass Transfer 24 (7) (1981) 1287–1291.
[10] M. Ouazzani, J. Platten, A. Mojtabi, Etude exprimentale de la convection mixte entre deux plans horizontaux tempratures diffrentes-ii, Int. J. Heat Mass Transfer 33 (7) (1990) 1417–1427.
[11] D. Goussis, R. Kelly, Surface wave and thermocapillary instabilities in a liquid film flow, J. Fluid Mech. 223 (1) (1991) 25–45.
[12] I. Sadiq, R. Usha, Linear instability in a thin viscoelastic liquid film on an inclined, non-uniformly heated wall, Int. J. Eng. Sci. 43 (19) (2005) 1435–1449.
[13] L. Bammou, K. El Omari, S. Blancher, Y. Le Guer, B. Benhamou, T. Mediouni, A numerical study of the longitudinal thermoconvective rolls in a mixed convection flow in a horizontal channel with a free surface, Int. J. Heat Fluid Flow 42 (2013) 265–277.
[14] O. Goncharova, O. Kabov, Mathematical and numerical modeling of convection in a horizontal layer under co-current gas flow, Int. J. Heat Mass Transf. 53 (13–14) (2010) 2795–2807.
[15] I.B. Simanovskii, A. Viviani, J.C. Legros, Buoyant–thermocapillary flows in a multilayer system, C. R. Mcanique 336 (3) (2008) 262–268.
[16] Z. Mao, P. Lu, G. Zhang, C. Yang, Numerical simulation of the Marangoni effect with interphase mass transfer between two planar liquid layers, Chin. J. Chem. Eng. 16 (2) (2008) 161–170.
[17] M. Medale, B. Cochelin, A parallel computer implementation of the asymptotic numerical method to study thermal convection instabilities, J. Comput. Phys. 228 (22) (2009) 8249–8262.
[18] J.R.A. Pearson, On convection cells induced by surface tension, J. Fluid Mech. 4 (05) (1958) 489–500.
[19] L.E. Scriven, C.V. Sternling, On cellular convection driven by surface-tension gradients: effects of mean surface tension and surface viscosity, J. Fluid Mech. 19 (03) (1964) 321–340.
[20] P. Laure, B. Roux, Linear and non-linear analysis of the Hadley circulation, J. Cryst. Growth 97 (1) (1989) 226–234.
[21] P.M. Parmentier, V.C. Regnier, G. Lebon, Buoyant–thermocapillary instabilities in medium-Prandtl-number fluid layers subject to a horizontal temperature gradient, Int. J. Heat Mass Transf. 36 (9) (1993) 2417–2427.
[22] J. Burguete, N. Mukolobwiez, F. Daviaud, N. Garnier, A. Chiffaudel, Buoyant–thermocapillary instabilities in extended liquid layers subjected to a horizontal temperature gradient, Phys. Fluids 13 (2001) 2773–2787.
[23] J.F. Mercier, C. Normand, Buoyant–thermocapillary instabilities of differentially heated liquid layers, Phys. Fluids 8 (1996) 1433–1445.
[24] H. Müller, M. Lücke, M. Kamps, Transversal convection patterns in horizontal shear flow, Phys. Rev. A 45 (6) (1992) 3714.
[25] H. Müller, M. Tveitereid, S. Trainoff, Rayleigh–Bénard problem with imposed weak through flow: two coupled Ginzburg–Landau equations, Phys. Rev. E. 48 (1) (1993) 263.
[26] M. Ouazzani, J. Platten, H. Müller, M. Lücke, Etude de la convection mixte entre deux plans horizontaux à températures différentes-iii, Int. J. Heat Mass Transfer 38 (5) (1995) 875–886.
[27] X. Nicolas, A. Mojtabi, J.K. Platten, Two-dimensional numerical analysis of the Poiseuille–Bénard flow in a rectangular channel heated from below, Phys. Fluids 9 (2) (1997) 337–348.
[28] P. Carrière, P.A. Monkewitz, Convective versus absolute instability in mixed Rayleigh–Bénard–Poiseuille convection, J. Fluid Mech. 384 (1999) 243–262.
[29] P.G. Drazin, W.H. Reid, Hydrodynamic Stability, Cambridge Univ. Press, Cambridge, 2004.
[30] C. Canuto, M. Hussaini, A. Quarteroni, T.A.J. Zang, Spectral Methods in Fluid Dynamics, Springer-Verlag, New York, 1987.
[31] L. Trefethen, Spectral methods in MATLAB, Vol. 10, Society for Industrial Mathematics, 2000.
[32] J.K. Platten, J.C. Legros, Convection in Liquids, Springer-Verlag, Berlin, 1984.
[33] P. Colinet, J. Legros, M. Velarde, I. Prigogine, Nonlinear Dynamics of Surface-Tension-Driven Instabilities, Wiley Online Library, 2001.
[34] P.J. Kundu, I.M. Cohen, Fluid Mechanics, Academic Press, 2002.